DOI: 10.1002/cjoc.201500268

A Silole-Based Efficient Electroluminescent Material with Good Electron-Transporting Potential

Changyun Quan,[a] Han Nie,[a] Rongrong Hu,[a] Anjun Qin,[a] Zujin Zhao,*,[a] and Ben Zhong Tang*,[a,b]

[a] *Guangdong Innovative Research Team, State Key Laboratory of Luminescent Materials and Devices, South China University of Technology, Guangzhou 510640, China*

[b] *Department of Chemistry, The Hong Kong University of Science & Technology, Clear Water Bay, Kowloon, Hong Kong, China*

A new silole derivative, 2,5-bis(7-(dimesitylboranyl)-9,9-dimethylfluoren-2-yl)-1-methyl-1,3,4-triphenylsilole ($(MesBF)_2MTPS$), is synthesized and characterized. $(MesBF)_2MTPS$ shows a good fluorescence efficiency of 15% in THF solution and a higher efficiency of 86% in solid film, presenting an aggregation-enhanced emission characteristic. It is thermally and morphologically stable, with high decomposition and glass-transition temperatures of 257 and 171 ℃, respectively. The LUMO energy level (–2.96 eV) of $(MesBF)_2MTPS$ is lower than that of TPBi, revealing its electron-transporting potential. Efficient organic light-emitting diodes (OLEDs) are fabricated using $(MesBF)_2MTPS$ as emitter, which radiates yellow light at 554 nm, and affords high maximum luminance, current efficiency, and external quantum efficiency of 48348 cd•m^{-2}, 12.3 cd•A^{-1}, and 4.1%, respectively.

Keywords silole, aggregation-enhanced emission, electroluminescence, electron transporter, organic light-emitting diodes

Introduction

In recent years, organic optoelectronic materials have drawn intense attention because of their various high-technological applications such as light emitters for organic light-emitting diodes (OLEDs).[1] Although considerable achievements have been made in the development of organic luminescent materials, major challenges still remain. One of main obstacle problems that urgently needs to be conquered is aggregation-caused quenching (ACQ) encountered by many conventional luminescent materials. In 2001, a novel phenomenon of aggregation-induced emission (AIE) was observed for siloles,[2,3] whose poor fluorescence property in solutions was ameliorated drastically as the aggregate formation. The important finding is helpful to alleviate the ACQ problem, and from then on, a large number of AIE-active luminogens were synthesized and studied. Many of them have high fluorescence efficiencies in solid films, and show great potential in OLEDs.[4,5]

Among numerous AIE luminogens,[6,7] siloles exhibit typical AIE effect with high fluorescence efficiencies in the aggregated state, and have a wide range of high-tech applications, such as chemosensors, bioprobes, and OLEDs.[8-10] Moreover, siloles own unique electron structure of σ*-π* conjugation between the σ* orbitals of two exocyclic silicon-carbon bonds and π* orbital of the butadiene moiety.[11-13] This characteristic endows them with low-lying LUMO energy levels and high electron affinity, making them promising candidates for electron-transporting and light-emitting layers in optoelectronic devices.[14,15] In this work, we designed and synthesized a novel silole derivative with bulky 9,9-dimethylfluorenyl and dimesitylboryl groups at the 2,5-positions of silole ring (Scheme 1), in order to develop efficient light emitters with good electron-transporting ability.[16-18] By studying the thermal, photophysical, electrochemical, and electroluminescent properties of the new silole, we find that it is an excellent solid-state light emitter and functions well as active layers in OLEDs.

Experimental

Materials and instruments

Anhydrous tetrahydrofuran was distilled from sodium and benzophenone under dry nitrogen immediately prior to use. All other chemicals and reagents were obtained from Aldrich and J&K Scientific Ltd, and used as received. ^{1}H and ^{13}C NMR spectra were recorded on a Bruker AV 400 spectrometer in deuterated dichloromethane using tetramethylsilane (TMS; $\delta=0$) as internal standard. UV spectra were measured on a Milton Roy Spectronic 3000 Array spectrophotometer. PL

* E-mail: mszjzhao@scut.edu.cn, tangbenz@ust.hk; Tel.: 0086-020-22237066
Received March 31, 2015; accepted May 27, 2015; published online June 12, 2015.

spectra were recorded on a Perkin-Elmer LS 55 spectrofluorometer. High resolution mass spectra (HRMS) were recorded on a GCT premier CAB048 mass spectrometer operating in MALDI-TOF mode. Thermogravimetric analysis (TGA) was carried on a TA TGA Q5000 under dry nitrogen at a heating rate of 10 ℃/min. Thermal transition was investigated by a TA DSC Q1000 under dry nitrogen at a heating rate of 10 ℃/min. The dynamic light scattering measurement was carried on Zetasizer Nano-ZS90.

Device fabrication

Glass substrates pre-coated with a 170 nm thin layer of indium tin oxide (ITO) with a sheet resistance of 10 Ω per square were thoroughly cleaned in ultrasonic bath of acetone, isopropyl alcohol, detergent, deionized water, and isopropyl alcohol and treated with O_2 plasma for 20 min in sequence. Organic layers were deposited onto the ITO-coated substrates by high-vacuum (<5×10^{-4} Pa) thermal evaporation. A 60 nm thin hole-transporting layer NPB was deposited. Next, a 20 nm (or 40 nm) thin $(MesBF)_2MTPS$ was deposited to form emitting layer (EML). Finally, a 40 nm (or 20 nm) thin electron-transporting layer (ETL) of TPBi was deposited to transport electrons, and to confine excitons in the emission zone. Cathodes, consisting of a 1 nm thin layer of LiF followed by a 100 nm thin layer of Al, were patterned using a shadow mask with an array of 3 mm×3 mm openings. Deposition rates are 1—2 A•s^{-1} for organic materials, 0.1 A•s^{-1} for LiF, and 6 A•s^{-1} for Al, respectively. EL spectra were taken by an optical analyzer, Photo Research PR705. The current density and luminance versus driving voltage characteristics were measured by Keithley 2420 and Konica Minolta chromameter CS-200, respectively.

Synthesis

(7-Bromo-9,9-dimethylfluoren-2-yl)dimesitylborane (2) *n*-Butyllithium (2.5 mol/L in hexane, 6.87 mL, 11 mmol) was added dropwise into a solution of 2,7-dibromo-9,9-dimethyl-9*H*-fluorene (5.63 g, 16 mmol) in dry THF (80 mL) at −78 ℃. After the mixture was stirred at −78 ℃ for 2 h, fluorodimesitylborane (2.68 g, 10 mmol) was added. After being warmed to room temperature and stirred for 6 h, the reaction was quenched with brine, and the aqueous layer was extracted with CH_2Cl_2 twice. The combined organic layers were dried over magnesium sulfate anhydrous. After filtration, the solvent was evaporated under reduced pressure, and the residue was purified by silica-gel column chromatography with *n*-hexane/dichloromethane as eluent. Compound **2** was obtained as a white solid in 80% yield. ^{1}H NMR (400 MHz, CD_2Cl_2) δ: 7.65—7.60 (m, 3H), 7.55 (d, J=8.0 Hz, 1H,), 7.52—7.50 (m, 1H), 7.47—7.45 (m, 1H), 6.83 (s, 4H), 2.33 (s, 6H), 2.02 (s, 12H), 1.43 (s, 6H); ^{13}C NMR (100 MHz, CD_2Cl_2) δ: 156.8, 152.6, 145.2, 141.8, 140.8, 138.5, 137.8, 136.3, 130.7, 130.1, 128.1, 126.2, 122.0, 121.9, 119.5, 47.4, 26.7, 23.5, 21.2. HRMS ($C_{33}H_{34}BBr$): 520.1937 [M+Na^+, calcd 543.1829].

2,5-Bis(7-(dimesitylboranyl)-9,9-dimethylfluoren-2-yl)-1-methyl-1,3,4-triphenylsilole ($(MesBF)_2MTPS$) The synthetic procedure was similar to that described in literature.[19] Yellow solid, yield 50%. ^{1}H NMR (400 MHz, CD_2Cl_2) δ: 7.71 (d, J=8.0 Hz, 2H), 7.53—7.49 (m, 4H), 7.46 (d, J=8.0 Hz, 2H), 7.42 (d, J=8.0 Hz, 2H), 7.38—7.34 (m, 3H), 7.05 (m, 6H), 6.97 (d, J=8.0 Hz, 2H), 6.94—6.92 (m, 4H), 6.83—6.80 (m, 8H), 6.77 (s, 2H), 2.30 (s, 12H), 1.98 (s, 24H), 1.10 (s, 12H), 0.88 (s, 3H); ^{13}C NMR (100 MHz, CD_2Cl_2) δ: 154.7, 153.3, 152.2, 143.4, 141.9, 140.9, 139.8, 139.6, 138.4, 138.2, 137.3, 135.2, 135.1, 133.6, 132.8, 129.6, 128.9,128.8, 127.2, 127.0, 126.6, 125.4, 122.6, 119.0, 118.1, 45.1, 25.4, 22.5, 20.2, −6.8. HRMS ($C_{89}H_{86}B_2Si$): 1204.6724 [M^+, calcd 1204.6685].

Scheme 1 Synthesis of $(MesBF)_2MTPS$

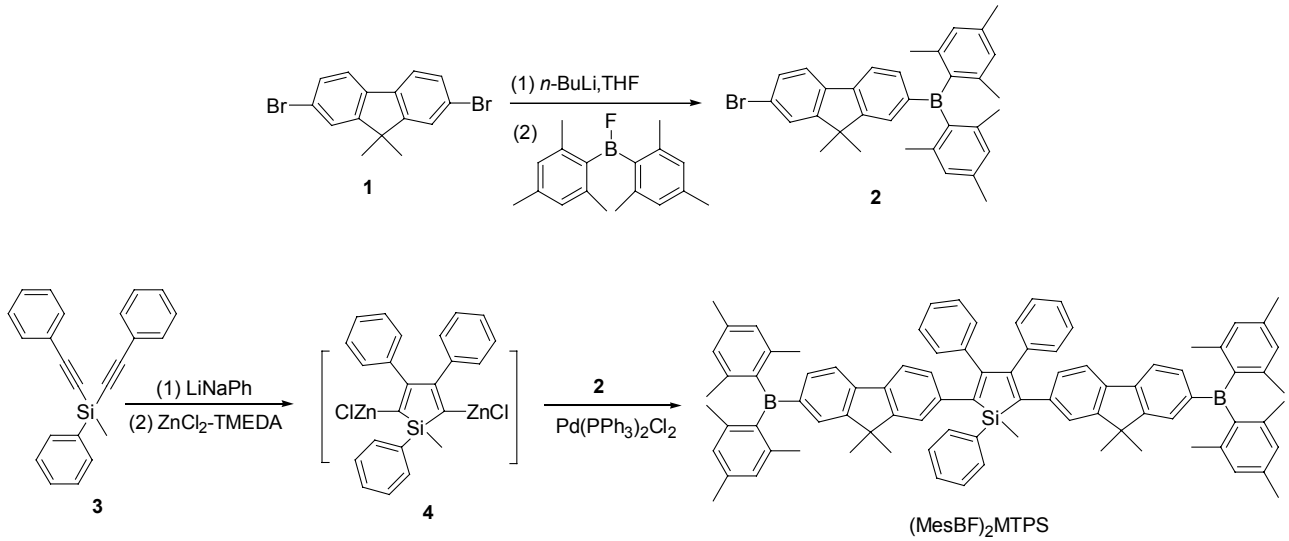

Reagents: LiNaph=lithium 1-naphthalenide; TMEDA=*N*,*N*,*N*′,*N*′-tetramethylethylenediamine.

Results and Discussion

Optical property

As shown in Figure 1A, the absorption maximum of $(MesBF)_2MTPS$ in THF solution appears at 411 nm, associated with π-π* transition. Its emission peak is located at 525 nm (Figure 1B), with a fluorescence quantum yield (Φ_F) of 15% (Figure 1D), measured by a calibrated integrating sphere. This value is much higher than those of the 2,3,4,5-tetraphenylsiloles in the literatures.[9,20] This is because the bulky substituents can lower the intramolecular rotation of the aromatic rotors around the silole ring,[21] and the radiative decay process in $(MesBF)_2MTPS$ is thus promoted, leading to a relatively high Φ_F value in solution. The emission intensity is further enhanced when a non-solvent of water is added into its THF solution (Figure 1C). Since $(MesBF)_2MTPS$ is insoluble in water, aggregates should have formed from $(MesBF)_2MTPS$ molecules in the mixtures with a high water fraction (f_w). The dynamic light scattering measurement reveals an average size of ~165 nm of the particle in the mixture with 90% water fraction (Figure S5). The emission enhancement caused by the aggregate formation is indicative of aggregation-enhanced emission (AEE) characteristic of the new silole. The solid film of $(MesBF)_2MTPS$ is more emissive, emitting at 535 nm with an excellent Φ_F value of 88% (Table 1). A small red shift of 10 nm is found in the PL spectrum of solid film relative to that in solution (Figure 1B). This should be ascribed to the dimesitylboryl groups, which lead to a branched molecular conformation, and thus, inhibit the strong intermolecular interactions.

Thermal stability

The thermal property of $(MesBF)_2MTPS$ was investigated by thermogravimetric analysis (TGA) and differential scanning calorimetry (DSC). The result shows that $(MesBF)_2MTPS$ has a good thermal stability with a decomposition temperature (T_d) of 257 ℃, according to 5% loss of initial weight. A high glass-transition temperature (T_g) of 171 ℃ (Table 1) is also detected,

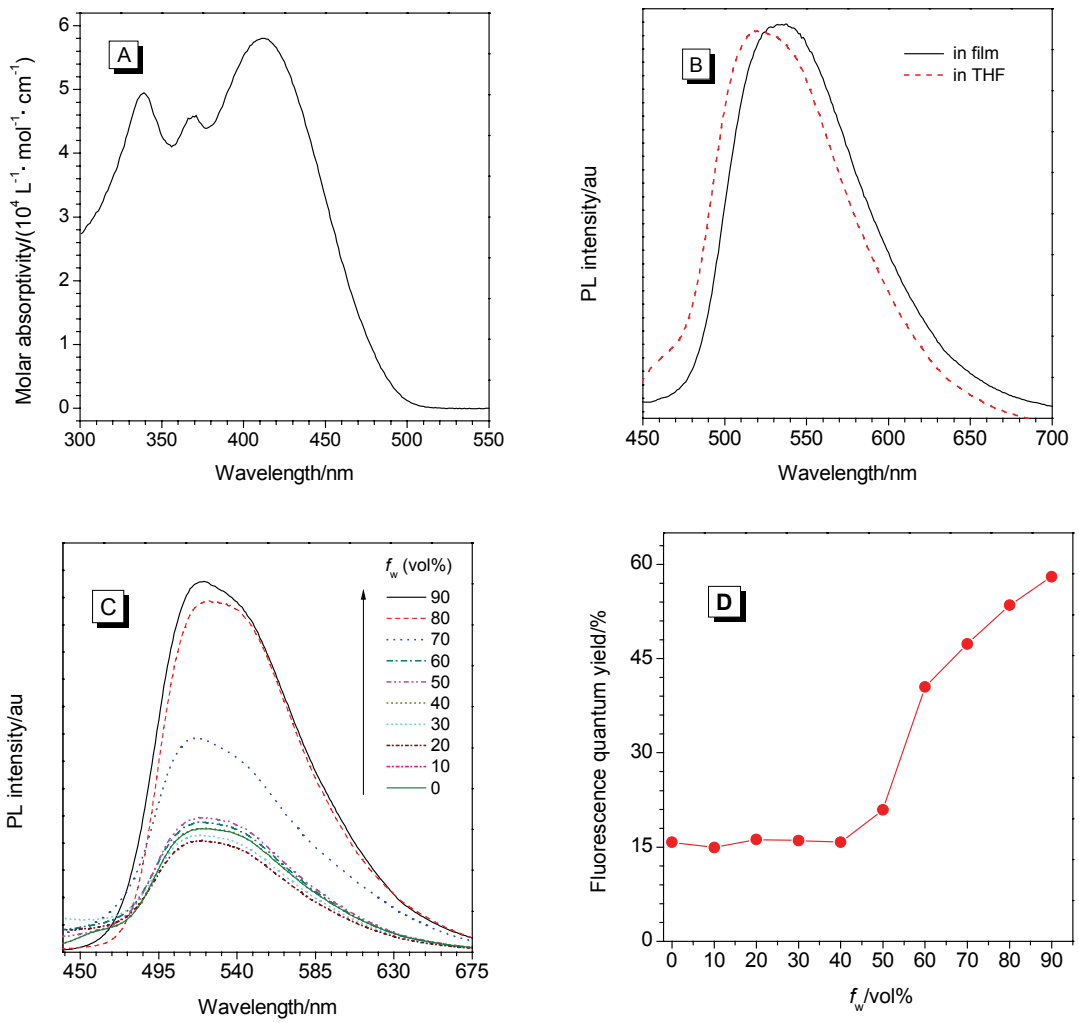

Figure 1 (A) Absorption spectrum of $(MesBF)_2MTPS$ in THF solution. (B) PL spectra of $(MesBF)_2MTPS$ in pure THF solution and in solid film. (C) PL spectra of $(MesBF)_2MTPS$ in THF/water mixtures with different water fractions (f_w, vol%). (D) Fluorescent quantum yields of $(MesBF)_2MTPS$ in THF/water mixtures with different water fractions. Excitation wavelength: 411 nm.

revealing it is morphologically stable. The good thermal property enables $(MesBF)_2MTPS$ to act as an active material for OLEDs fabricated by vacuum-deposition technique.

Electrochemical property

The electrochemical property of $(MesBF)_2MTPS$ was investigated by cyclic voltammetry (CV) in acetonitrile solution with 0.1 mol/L tetrabutylammonium hexafluorophosphate as supporting electrolyte at a scan rate of 50 mV•s^{-1}, using platinum as the working electrode and saturated calomel electrode (SCE) as the reference electrode. The CV curve is presented in Figure 2. The oxidation onset potential (E_{onset}) of $(MesBF)_2MTPS$ occurs at –1.12 eV. Hence, the HOMO energy level is calculated to be –5.52 eV [HOMO=–(4.4+E_{onset})], and the LUMO energy level is determined as –2.96 eV from the optical band gap energy (E_g) and the HOMO value (LUMO=–(HOMO+E_g)).[22] The LUMO energy level of the $(MesBF)_2MTPS$ is lower than that of TPBi (–2.7 eV), implying the potential as electron transporting material for OLEDs.

Electroluminescence

The excellent solid-state fluorescence efficiency and good thermal stability of $(MesBF)_2MTPS$ encouraged us to investigate its electroluminescence (EL) property. Triple-layer OLED with a configuration of ITO/NPB (60 nm)/$(MesBF)_2MTPS$ (20 nm)/TPBi (40 nm)/LiF (1 nm)/Al (100 nm) (Device I) was fabricated, in which the $(MesBF)_2MTPS$ acted as a light-emitting layer, *N*,*N*-bis-(1-naphthyl)-*N*,*N*-diphenylbenzidine (NPB) functioned as a hole-transporting layer, and 1,3,5-tris(*N*-phenylbenzimiazole-2-yl)-benzene (TPBi) served as an electron-transporting layer. The device performance data are listed in Table 2, and the EL spectra and characteristic curves of the devices are shown in Figure 3. The device shows yellow light with emission maximum located at 554 nm, which is red-shifted by 19 nm in comparison with its PL in solid film. The device is turned on at 3.8 V, and gives high maximum luminance, current efficiency, and external quantum efficiency of 48348 cd•m^{-2}, 12.3 cd•A^{-1}, and 4.1%, respectively. Concerning the low-lying LUMO of $(MesBF)_2MTPS$ that may improve its electron-transporting ability, an additional device (device II) was fabricated, in which the thickness of TPBi was decreased to 20 nm and the thickness of light-emitting layer was increased to 40 nm. The device II also shows good performance, with a high maximum luminance, current efficiency, and external quantum efficiency of 34080 cd•m^{-2}, 10.1 cd•A^{-1}, and 3.3%, respectively, demonstrating that $(MesBF)_2MTPS$ has great potential to function as both light emitter and electron transporter in OLEDs.

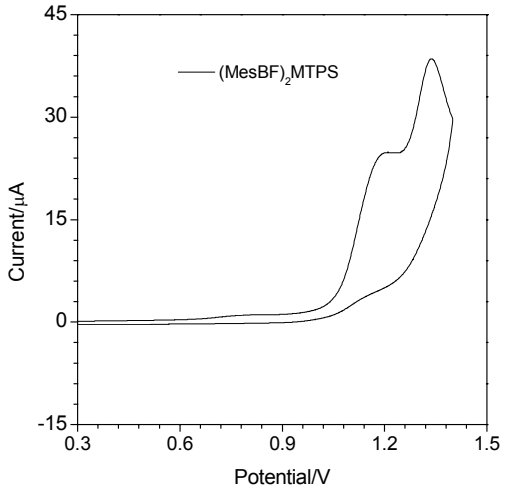

Figure 2 Cyclic voltammogram of $(MesBF)_2MTPS$ measured in acetonitrile containing 0.1 mol/L tetrabutylammonium hexafluorophosphate. Scant rate: 50 mV•s^{-1}.

Conclusions

A new silole derivative $(MesBF)_2MTPS$ with bulky substituents was synthesized and fully characterized. Introduction of fluorescent 9,9-dimethylfluorenyl and dimesitylboryl into the 2,5-positions of silole ring makes silole AEE-active. Efficient triple-layer device is achieved using $(MesBF)_2MTPS$ as light-emitting layer, giving good EL performance of 48348 cd•m^{-2}, 12.3

Table 1 Optical, electronic and thermal properties of $(MesBF)_2MTPS$

Compound	λ_{abs}[a]/nm	λ_{em}[b]/nm		Φ_F[c]/%		(T_g/℃)/(T_d/℃)	(HOMO/eV)/(LUMO/eV)	E_g/eV
		Soln	Film	Soln	Film			
$(MesBF)_2MTPS$	411	525	535	15	88	171/257	–5.52/–2.96	2.56

[a] Absorption maximum in dilute THF solution (10 μmol/L). [b] Emission maximum in THF solution (Soln) or in solid film. [c] Absolute fluorescence quantum yield in THF solution or in solid film, measured by a calibrated integrating sphere.

Table 2 EL performance of OLEDs based on $(MesBF)_2MTPS$[a]

Device	λ_{EL}/nm	V_{on}/V	L/(cd•m^{-2})	η_C/(cd•A^{-1})	η_P/(lm•W^{-1})	EQE	CIE (x, y)
I	554	3.8	48348	12.3	8.8	4.1	(0.41, 0.56)
II	554	4.6	34080	10.1	5.9	3.3	(0.41, 0.56)

[a] The luminescence (L), current efficiency (η_c), power efficiency (η_P) and external quantum efficiency (EQE) are the maximum values of the devices. V_{on} is defined as the voltage required for 1 cd•m^{-2}. Device configuration: ITO/NPB (60 nm)/$(MesBF)_2MTPS$ (20 nm)/TPBi (40 nm)/LiF (1 nm)/Al (100 nm) (Device I); ITO/NPB (60 nm)/$(MesBF)_2MTPS$ (40 nm)/TPBi (20 nm)/LiF (1 nm)/Al (100 nm) (Device II).

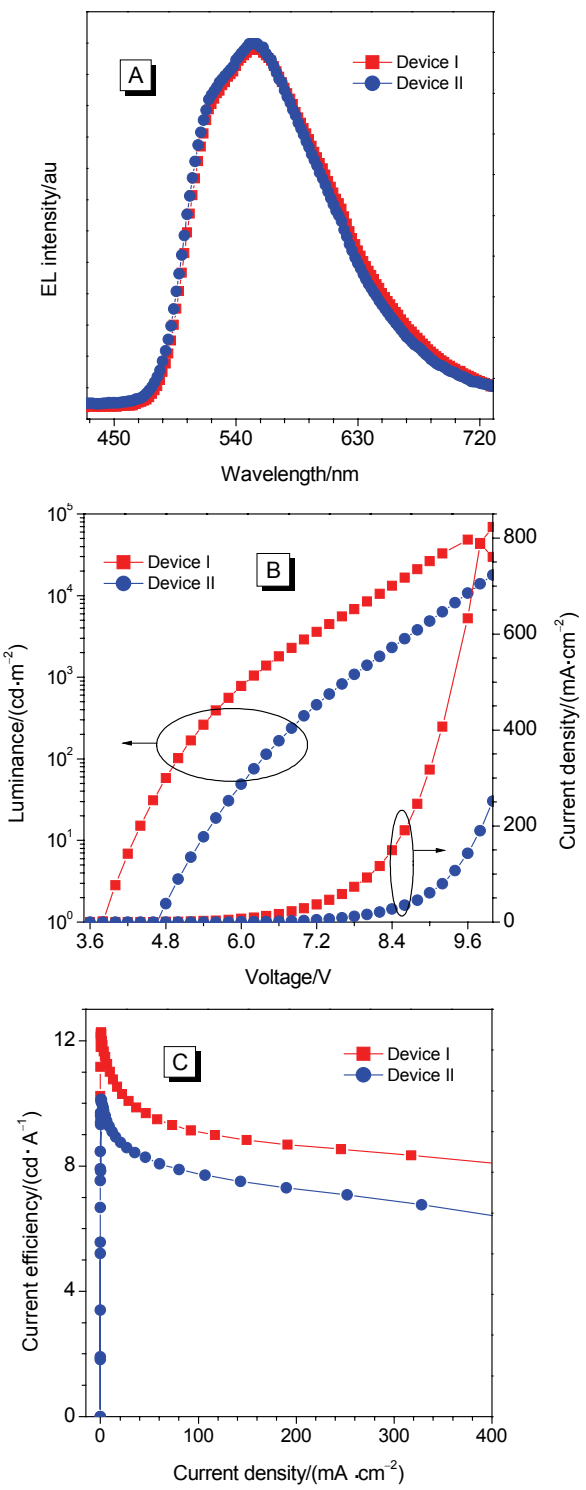

Figure 3 (A) EL spectra, (B) current density-voltage-luminance characteristics, and (C) plots of current efficiency versus current density of devices based on $(MesBF)_2$MTPS. Device configuration: ITO/NPB (60 nm)/$(MesBF)_2$MTPS (20 nm)/TPBi (40 nm)/LiF (1 nm)/Al (100 nm) (Device I); ITO/NPB (60 nm)/$(MesBF)_2$MTPS (40 nm)/TPBi (20 nm)/LiF (1 nm)/Al (100 nm) (Device II).

cd•A^{-1}, and 4.1%. In addition, owing to the low-lying LUMO, the $(MesBF)_2$MTPS can partially replace TPBi to serve as electron transporter. The further development of silole-based materials that can efficiently function as both light emitter and electron transporter is in progress.

Acknowledgement

We acknowledge the financial support from the National Natural Science Foundation of China (51273053), the Guangdong Natural Science Funds for Distinguished Young Scholar (No. 2014A030306035), the Guangdong Innovative Research Team Program of China (No. 201101C0105067115), the National Basic Research Program of China (973 Program, Nos. 2015CB655000 and 2013CB834702) and the Fundamental Research Funds for the Central Universities.

References

[1] Tang, C.; VanSlyke, S. *Appl. Phys. Lett.* **1987**, *51*, 913.
[2] Luo, J.; Xie, Z.; Lam, J. W. Y.; Cheng, L.; Chen, H.; Qiu, C.; Kwok, H. S.; Zhan, X.; Liu, Y.; Zhu, D.; Tang, B. Z. *Chem. Commun.* **2001**, 1740.
[3] Mei, J.; Hong, Y.; Lam, J. W. Y.; Qin, A.; Tang, Y.; Tang, B. Z. *Adv. Mater.* **2014**, *26*, 5429.
[4] Ma, S. Q.; Zhang, J. B.; Chen, J. L.; Wang, L. J.; Xu, B.; Tian, W. J. *Chin. J. Chem.* **2013**, *31*, 1418.
[5] Zhao, Z.; Chen, S.; Lam, J. W. Y.; Lu, P.; Zhong, Y.; Wong, K. S.; Kwok, H. S.; Tang, B. Z. *Chem. Commun.* **2010**, *46*, 2221.
[6] Li, H.; Chi, Z.; Xu, B.; Zhang, X.; Yang, Z.; Li, X.; Liu, S.; Zhang, Y.; Xu, J. *J. Mater. Chem.* **2010**, *20*, 6103.
[7] Shimizu, M.; Mochida, K.; Hiyama, T. *Angew. Chem., Int. Ed.* **2008**, *47*, 9760.
[8] Heng, L.; Dong, Y.; Zhai, J.; Tang, B. Z.; Jiang, L. *Langmuir* **2008**, *24*, 2157.
[9] Liu, J.; Lam, J. W. Y.; Tang, B. Z. *J. Inorg. Organomet. Polym. Mater.* **2009**, *19*, 249.
[10] Tracy, H. J.; Mullin, J. L.; Klooster, W. T.; Martin, J. A.; Haug, J.; Wallace, S.; Rudloe, I.; Watts, K. *Inorg. Chem.* **2005**, *44*, 2003.
[11] Wrackmeyer, B.; Kehr, G.; Suss, J.; Molla, E. *J. Organomet. Chem.* **1999**, *577*, 82.
[12] Wang, M.; Zhang, G.; Zhang, D.; Zhu, D.; Tang, B. Z. *J. Mater. Chem.* **2010**, *20*, 1858.
[13] Zhao, Z.; Liu, D.; Lam, J. W. Y.; Lu, P.; Yang, B.; Ma, Y.; Tang, B. Z. *Sci. China Chem.* **2010**, *53*, 2311.
[14] Tamao, K.; Uchida, M.; Izumizawa, T.; Furukawa, K.; Yamaguchi, S. *J. Am. Chem. Soc.* **1996**, *118*, 11974.
[15] Murata, H.; Kafafi, Z. H.; Uchida, M. *Appl. Phys. Lett.* **2002**, *80*, 189.
[16] Jia, W. L.; Moran, M. J.; Yuan, Y. Y.; Lu, Z. H.; Wang, S. *J. Mater. Chem.* **2005**, *15*, 3326.
[17] Li, D.; Zhang, H.; Wang, C.; Huang, S.; Guo, J.; Wang, Y. *J. Mater. Chem.* **2012**, *22*, 4319.
[18] Xu, X.; Ye, S.; He, B.; Chen, B.; Xiang, J.; Zhou, J.; Lu, P.; Zhao, Z.; Qiu, H. *Dyes Pigm.* **2014**, *101*, 136.
[19] Zhang, T. T.; Zhu, C. Q.; Ma, Y. W.; Wang, C. Y.; Shen, Y. J. *Chin. J. Chem.* **2013**, *31*, 779
[20] Zhao, Z.; Wang, Z.; Lu, P.; Chan, C. Y. K.; Liu, D.; Lam, J. W. Y.; Sung, H. H. Y.; Williams, I. D.; Ma, Y.; Tang, B. Z. *Angew. Chem., Int. Ed.* **2009**, *48*, 7608.
[21] Chen, B.; Jiang, Y.; Chen, L.; Nie, H.; He, B.; Lu, P.; Sung, H. H. Y.; Williams, I. D.; Kwok, H. S.; Qin, A.; Zhao, Z.; Tang, B. Z. *Chem. Eur. J.* **2014**, *20*, 1931.
[22] Li, Y.; Cao, Y.; Gao, J.; Wang, D.; Yu, G.; Heeger, A. J. *Synth. Met.* **1999**, *99*, 243.

(Pan, B.; Qin, X.)

